Available online at www.sciencedirect.com
ScienceDirect
Trans. Nonferrous Met. Soc. China 27(2017) 2415−2422
Transactions of Nonferrous Metals Society of China
www.tnmsc.cn

Calculation and experimental study on heating temperature field of super-high strength aluminum alloy thick plate

Shi-tong FAN[1], Yun-lai DENG[1,2], Jin ZHANG[3], Xiao-bin GUO[1]

1. School of Materials Science and Engineering, Central South University, Changsha 410083, China;
2. State Key Laboratory of High Performance and Complex Manufacturing, Central South University, Changsha 410083, China;
3. Light Alloy Research Institute, Central South University, Changsha 410083, China

Received 15 July 2016; accepted 22 May 2017

Abstract: Stepped heating treatment has been applied to aluminum alloy thick plate to improve the mechanical performance and corrosion resistance. Accurate temperature control of the plate is the difficulty in engineering application. The heating process, the calculation of surface heat transfer coefficient and the accurate temperature control method were studied based on measured heating temperature for the large-size thick plate. The results show that, the temperature difference between the surface and center of the thick plate is small. Based on the temperature uniformity, the surface heat transfer coefficient was calculated, and it is constant below 300 °C, but grows greatly over 300 °C. Consequently, a lumped parameter method (LPM) was developed to predict the plate temperature. A stepped solution treatment was designed by using LPM, and verified by finite element method (FEM) and experiments. Temperature curves calculated by LPM and FEM agree well with the experimental data, and the LPM is more convenient in engineering application.

Key words: lumped parameter method; surface heat transfer coefficient; temperature field; aluminum alloy; thick plate

1 Introduction

The importance of temperature fields in heat treatment of aluminum thick plate is indisputable. The key parameters in any heat treatment are time and temperature, which ideally depend on the diffusion of alloying elements [1]. Due to the importance of temperature fields in microstructure, they influence the mechanical and corrosive properties of aluminum alloys directly. So, searching for a direct method to calculate the temperature fields of thick plates is important.

Nowadays, stepped heat treatment is a development trend of aluminum and paid more and more attention. Stepped heat treatment was first used in aging treatment, known as retrogression and re-aging (RRA), which was first applied to 7075 alloy in T6 condition, involving a short heat treatment in the temperature range of 200−280 °C followed by T6 re-aging [2,3]. Then, considerable research has been conducted on it, and it is proved as an advanced aging treatment leading to a favorable combination of good strength and stress-corrosion cracking resistance [4−7]. In recent years, stepped treatments in homogenization [8], solution [9] and quenching [10] have gradually become research hotspots. DENG et al [11] studied the two-stage homogenization scheme of 7085 alloy, and demonstrated that more homogeneous Al_3Zr particles may be nucleated at the grain boundary in the first low-temperature stage. CHEN et al [12] studied both the stepped homogenization and advanced solution of 7055 alloy, and revealed that a suitable pretreatment could enable a complete dissolution of η phase, leading to better mechanical properties. HAN et al [13] reported the advanced solution of 7050 alloy, which resulted in smaller sub-grains than the single-stage solution, and higher strength and fracture toughness. XU et al [14] used both advanced solution and RRA, and the obtained samples showed better mechanical properties for the higher volume fractions of η' and η precipitates.

Foundation item: Project (2012CB619500) supported by the National Basic Research Program of China; Project (51375503) supported by the National Natural Science Foundation of China; Project (2016YFB0300901) supported by the Major State Research Program of China; Project (2013A017) supported by the Bagui Scholars Program of Guangxi Zhuang Autonomous Region, China

Corresponding author: Yun-lai DENG; Tel: +86-13873152095; E-mail: luckdeng@csu.edu.cn

DOI: 10.1016/S1003-6326(17)60268-1

However, almost all these heat treatments strongly depend on the accurate control of the material temperature. In these studies, the temperature differences between the samples and the surrounding are ignored for the insignificant small size of the samples. But in practice, based on the measured single-stage surface heating curve of 7050 thick plate (180 mm in thickness) in our previous work (see Fig. 1), we found the heating speed of the metals may be far below the surrounding because of the low surface heat transfer coefficient and the large volume. And for the more complex stepped heat treatment, the traditional heating method would be completely inappropriate.

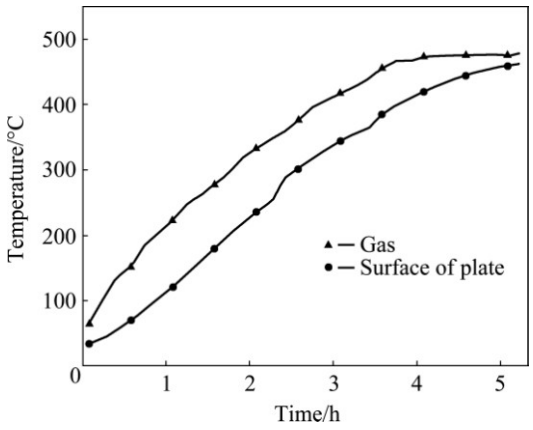

Fig. 1 Measured heating curve of 7050 thick plate (180 mm in thickness)

In this work, the heating manner was studied with a 7050 super-high strength aluminum thick plate. Based on the measured heating data, the temperature uniformity was discussed, and the variation of surface heat transfer coefficient along with the plate temperature was greatly concerned. Furthermore, the equation of thick plate temperature was given with the linear changing of the gas temperature. At last, a feasible heating method for stepped solution treatment was designed to verify the results.

2 Experimental

A 7050 aluminum alloy thick plate with a nominal composition of Al−2.2Cu−2.0Mg−6.5Zn−0.12Zr−0.05Ti (mass fraction, %) was chosen for the investigation. The dimensions were 1300 mm × 1100 mm × 180 mm. In order to measure the temperature in different thicknesses, drills were bored on the side face with the depth of 200 mm. The distances between the holes and the surface are 5, 15, 30, 60 and 90 mm, respectively. Then, K-type thermocouples were inserted into the bottom of the holes, which were filled with asbestos to prevent the heat flux. The temperature measurement facility is illustrated in Fig. 2.

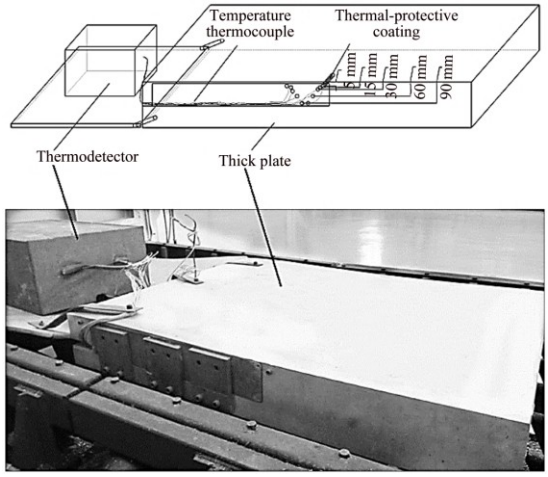

Fig. 2 Illustration of temperature measurement and real device

3 Results and discussion

Heating the gas to 470 °C directly in a resistance furnace, the heating curves in different thicknesses of 7050 plate with 180 mm in thickness are shown in Fig. 3, which reveals that the plate temperature is almost uniform in furnace heating condition, and this is quite different from steel. Temperature uniformity will be discussed in the following, and the actual surface transfer coefficient will be calculated based on it.

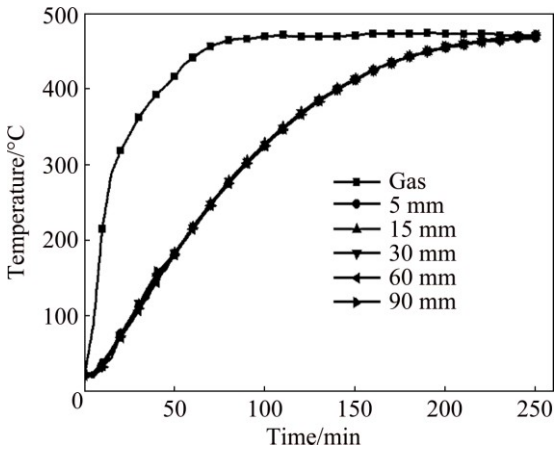

Fig. 3 Heating curves in different thicknesses of 7050 plate

3.1 Temperature uniformity

The temperature uniformity of the thick plate depends on the factors such as, plate thickness ($2l$), surface and center temperatures (T_w and T_c), gas temperature (T_f), surface heat transfer coefficient (h) and heat conductivity coefficient (k). Figure 4 shows the schematic diagram of the thick plate heating. The surface transfer heat flux is equal to the plate heat flux of conduction:

$$hA_{top}(T_f - T_w) = kA_{top}(T_w - T_c)/l \quad (1)$$

where A_{top} is the area of the top face.

The surface thermal resistance (R_w) is the reciprocal of the surface heat transfer coefficient $R_w=1/h$, and the plate thermal resistance from the surface to the center (R_c) is calculated as the ratio of mid thickness to heat conductivity coefficient $R_c=l/k$.

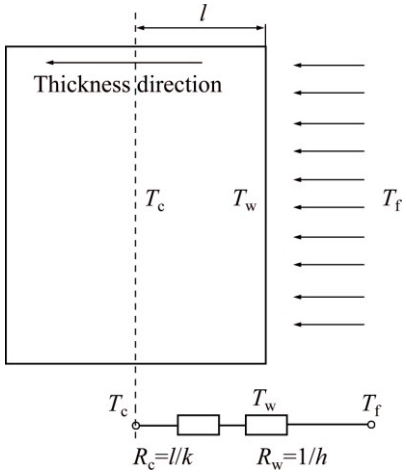

Fig. 4 Schematic diagram of thick plate heating

Equation (1) then becomes

$$\frac{T_w-T_c}{R_c}=\frac{T_f-T_w}{R_w} \tag{2}$$

T_w-T_c is the temperature difference between the surface and the center, and it can be estimated by Eq. (2). Obviously, smaller plate thermal resistance and larger surface thermal resistance would decrease the temperature difference. In resistance furnace, the surface transfer coefficient (h) is 10−100 W/(m^2·K), namely the minimum surface thermal resistance (R_w) is 0.01 m^2·K/W. For 7050 thick plate (180 mm in thickness), the plate thermal resistance (R_c) is only 0.001 m^2·K/W. With the measured heating curves shown in Fig. 3, the maximum temperature difference T_w-T_c of the plate is estimated in Fig. 5.

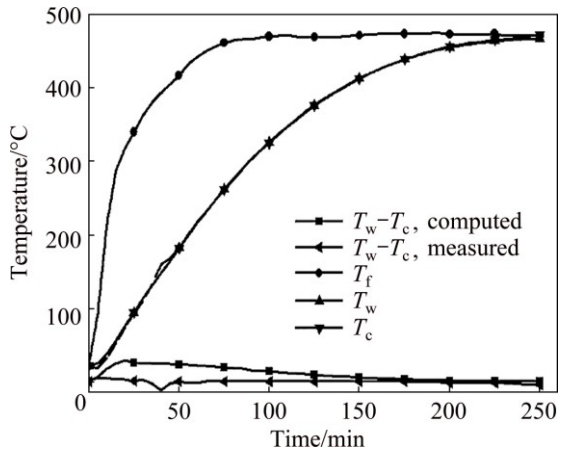

Fig. 5 Temperature difference between surface and center

Figure 5 shows that the maximum calculated temperature difference (22 °C) exists at the beginning of heating process, and decreases as the temperature rises. But in fact, the measured temperature difference is much smaller and almost zero in the whole process because the actual surface thermal resistance is much larger than the minimum value used in calculation. So, for aluminum thick plate (thickness below 180 mm), the temperature can be considered as uniform in furnace heating ($T_f-T_w\leq$300 °C).

3.2 Calculation of surface heat transfer coefficient

The surface heat transfer coefficient of plate cannot be measured directly, but can be calculated by measured heating curves. When the temperature fields of any time are known, it can be calculated based on the principle of energy balance, namely heat absorbed by the plate is equal to the heat transfer on the surface.

Within $t-\Delta t$ to t, heat absorbed by the plate (φ) can be calculated as a function of its rise in temperature:

$$\varphi=2c_p\rho A_{top}\int_0^l(T_t-T_{t-\Delta t})\mathrm{d}l \tag{3}$$

where c_p is the specific thermal capacity of the plate; ρ is the plate's density; T_t and $T_{t-\Delta t}$ are the temperature fields at the t and $t-\Delta t$ moments, respectively.

Considering $\int_0^l(T_t-T_{t-\Delta t})\mathrm{d}l=S$, Eq. (3) then becomes

$$\varphi=2c_p\rho A_{top}S \tag{4}$$

Within $t-\Delta t$ to t, heat transfer on the surface (φ) can be calculated as a function of the temperature difference between the gas and the surface:

$$\varphi=h_{t-\Delta t}A\int_{t-\Delta t}^t(T_f-T_w)\mathrm{d}t \tag{5}$$

where $h_{t-\Delta t}$ is the surface heat transfer coefficient at the $t-\Delta t$ moment, A is the surface of the plate.

Considering $\int_{t-\Delta t}^t(T_f-T_w)\mathrm{d}t=P$, Eq. (5) then becomes

$$\varphi=h_{t-\Delta t}AP \tag{6}$$

From Eq. (4) to Eq. (6), the surface heat transfer coefficient at the $t-\Delta t$ moment is given by

$$h_{t-\Delta t}=\frac{2c_p\rho A_{top}S}{AP} \tag{7}$$

As stated in Section 3.1, the temperature of aluminum thick plate is uniform. Meanwhile, due to the slow heating speed of thick plate, when Δt is small enough, the gas temperature (T_f) and the plate temperature (T) can be taken as constant.

So, $S=\int_0^l (T_t-T_{t-\Delta t})\mathrm{d}l=(T_t-T_{t-\Delta t})l$,

and $P=\int_{t-\Delta t}^{t}(T_\mathrm{f}-T_\mathrm{w})\mathrm{d}t=(T_\mathrm{f}-T_{t-\Delta t})\Delta t$.

Therefore, Eq. (7) becomes

$$h_{t-\Delta t}=\frac{2c_p\rho A_{\mathrm{top}}(T_t-T_{t-\Delta t})l}{A(T_\mathrm{f}-T_{t-\Delta t})\Delta t} \tag{8}$$

Based on the measured heating curves shown in Fig. 3, the surface heat transfer coefficient is calculated with Eq. (8). Meanwhile, according to the relationship between plate temperature and time, the correlation between the surface heat transfer coefficient and plate temperature is illustrated in Fig. 6. It shows that the surface heat transfer coefficient is very small and changes little when the temperature is below 300 °C, while it increases sharply when the temperature is over 300 °C.

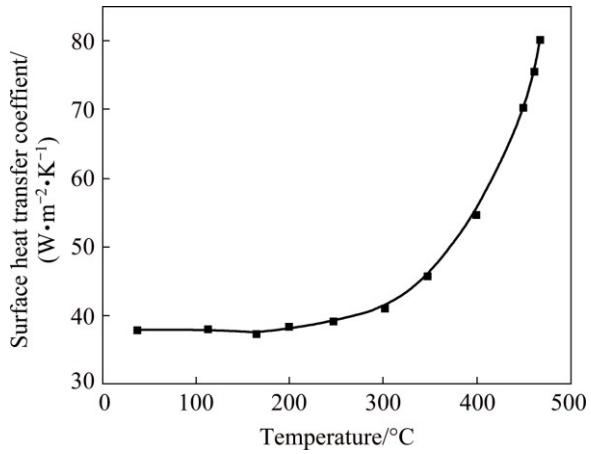

Fig. 6 Relationship between surface heat transfer coefficient and plate temperature

4 Calculation of aluminum thick plate temperature

4.1 Calculation of surface heat transfer coefficient

The heat transfer on the surface includes forced convection heat transfer in gas and radiant heat transfer in the furnace. From Newton's law of cooling and Stefan−Boltzmann law, the heat transferred on the surface (Q) can be expressed as

$$Q=Q_\mathrm{w}+Q_\mathrm{r} \tag{9}$$

$$Q_\mathrm{w}=h_\mathrm{w}A(T_\mathrm{f}-T_\mathrm{w}) \tag{10}$$

$$Q_\mathrm{r}=\xi C_0 A[(T_\mathrm{f}+273.15)^4-(T_\mathrm{w}+273.15)^4] \tag{11}$$

where Q_w is the forced convection transferred heat; Q_r is the radiant heat; h_w is the convection heat transfer coefficient; ξ is the emissivity of the plate; and C_0 is Stefan−Boltzmann constant 5.6695×10^{-8} W/(m^2·K^4).

To give a unified representation to the surface heat transfer coefficient (h), the radiant heat transfer coefficient (h_r) can be expressed as

$$h_\mathrm{r}=\frac{Q_\mathrm{r}}{A_{\mathrm{total}}(T_\mathrm{f}-T_\mathrm{w})}=\frac{\xi C_0[(T_\mathrm{f}+273.15)^4-(T_\mathrm{w}+273.15)^4]}{T_\mathrm{f}-T_\mathrm{w}} \tag{12}$$

And the surface heat transfer coefficient can be expressed as

$$h=h_\mathrm{w}+h_\mathrm{r} \tag{13}$$

4.1.1 Convection heat transfer coefficient

The convection heat transfer coefficient can be calculated with the characteristic number equation [15]:

$$h_\mathrm{w}=0.664(vm/\eta)^{1/2}Pr^{1/3}\lambda/m=0.664(\eta^{-1/2}Pr^{1/3}\lambda)\left(\frac{v}{m}\right)^{1/2} \tag{14}$$

where λ is the gas heat conductivity coefficient; Pr is the Prandtl number of gas; η is the air dynamic viscosity; v is the air velocity in the furnace; m is the characteristic length of plate.

In a specific furnace, v is the air velocity of the heating circulator, and m is equal to the heating nozzle space, and both of which are constant. So, the surface heat transfer coefficient is determined by the value of $\eta^{-1/2}Pr^{1/3}\lambda$, which changes with the temperature. With the values of η, Pr and λ at different temperatures, the values of $\eta^{-1/2}Pr^{1/3}\lambda$ are calculated and shown in Fig. 7. Obviously, the variation of $\eta^{-1/2}Pr^{1/3}\lambda$ is small, and the average value is 5.82 W·s$^{1/2}$/(K·m^2).

Therefore, Eq. (14) becomes

$$h_\mathrm{w}=3.884\left(\frac{v}{m}\right)^{1/2} \tag{15}$$

The air velocity (v) in the furnace in this study is 30 m/s, and the characteristic length (m) is 0.325 m, so the forced convection heat transfer coefficient (h_w) calculated with Eq. (15) is 37.5 W/(m^2·K).

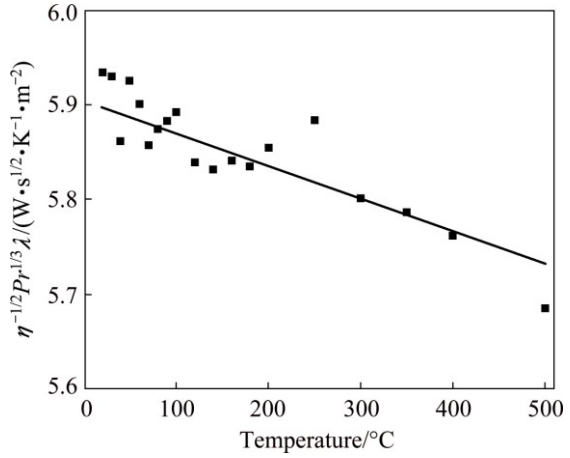

Fig. 7 Values of $\eta^{-1/2}Pr^{1/3}\lambda$ at different temperatures

4.1.2 Radiant heat transfer coefficient

The radiant heat transformation is determined by the emissivity (ξ) of the plate, which is greatly influenced by the plate temperature. The emissivity is very small when the temperature is low, but it rises greatly with elevating temperature. By using Eqs. (9)−(11) and the measured heating curves, the emissivity is calculated and shown in Fig. 8. The relationship between the emissivity and the plate temperature can be exactly fitted with exponential function:

$$\xi=0.01+1.52\times10^{-3}\exp(T/81.88) \tag{16}$$

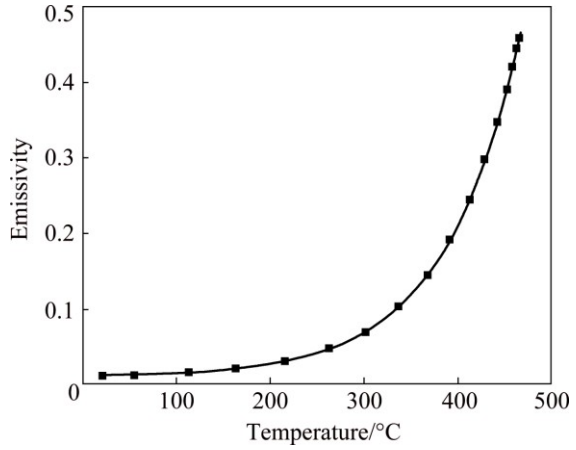

Fig. 8 Variation of emissivity with plate temperature

4.1.3 Change rules of surface heat transfer coefficient

From Eqs. (12), (13) and (15), the surface heat transfer coefficient is given by

$$h=3.884\left(\frac{v}{m}\right)^{1/2}+\frac{\xi C_0[(T_\mathrm{f}+273.15)^4-(T_\mathrm{w}+273.15)^4]}{T_\mathrm{f}-T_\mathrm{w}}=3.884\left(\frac{v}{m}\right)^{1/2}+\xi C_0[(T_\mathrm{f}+273.15)^2+(T_\mathrm{w}+273.15)^2](T_\mathrm{f}+T_\mathrm{w}+556.3) \tag{17}$$

Equation (17) shows that the surface heat transfer coefficient is related to both the gas temperature and the plate temperature, and the calculation becomes complex. However, due to the low temperature (almost below 530 °C) of aluminum heat treatment, Eq. (17) can be simplified appropriately. Figure 8 indicates that the emissivity is very small when the plate temperature is below 300 °C, so the impact on the coefficient of substituting T_f with T_w is insignificant in Eq. (17). Meanwhile, when the plate temperature is over 300 °C, the temperature difference between T_f and T_w is low, and the T_f can also be substituted with T_w. Meanwhile, as the aluminum thick plate temperature is uniform, T_w can be substituted with T.

Then, Eq. (17) becomes

$$h=3.884\left(\frac{v}{m}\right)^{1/2}+4\xi C_0(T+273.15)^3 \tag{18}$$

The surface heat transfer coefficient calculated from Eq. (18) is compared with the actual data, as shown in Fig. 9, which indicates that the calculating precision is very high. The results also show that the surface heat transfer coefficient is small and changes little when the temperature is below 300 °C, and the value is about 37.5 W/(m^2·K), which is equal to the convection heat transfer coefficient. When the temperature is over 300 °C, the coefficient increases greatly because of the radiation.

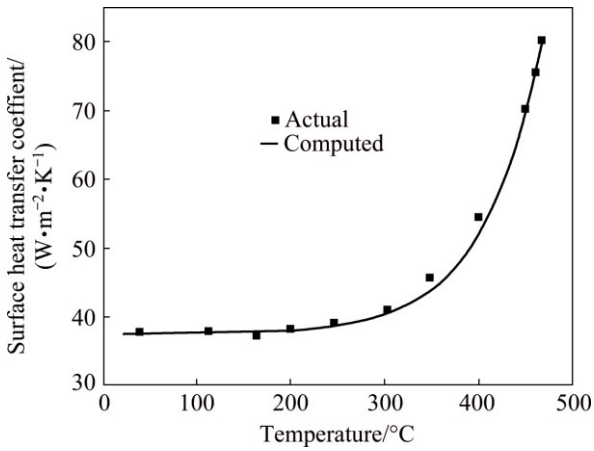

Fig. 9 Comparison of calculated surface heat transfer coefficient and actual data

4.2 Calculation of thick plate temperature

Since the surface heat transfer coefficient is given by Eq. (18), the plate temperature can be calculated by finite element method. Furthermore, as the temperature is considered as uniform in aluminum thick plate, it can also be calculated by lumped parameter method (LPM), and only the gas temperature is needed to consider in the calculation.

Assuming that the gas temperature rises linearly, the calculation of plate temperature by LPM is discussed in the following. If the initial temperature of the plate is T_0, the relationship between the plate and the gas at any time is given as

$$\rho c_p V\frac{\mathrm{d}T}{\mathrm{d}t}=hA(T_\mathrm{f}-T) \tag{19}$$

where V is the volume of the plate.

The gas temperature is expressed as

$$T_\mathrm{f}=T_0+bt \tag{20}$$

where b is the gas heating velocity.

By introducing the excess temperature of plate $\theta=T-T_0$, Eq. (19) then becomes

$$\frac{\rho c_p V}{hA}\frac{\mathrm{d}\theta}{\mathrm{d}t}=bt-\theta \tag{21}$$

The initial conditions are t=0, θ=0. Assuming that the surface heat transfer coefficient has no change with temperature, the analytic solution of Eq. (21) is given by

$$\theta=\frac{b\rho c_p V}{hA}\exp[-hAt/(\rho c_p V)]+b\left(t-\frac{\rho c_p V}{hA}\right) \tag{22}$$

Mathematically,

$$T=bt-\frac{b\rho c_p V}{hA}[1-\exp(-hAt/(\rho c_p V))]+T_0=$$
$$T_\mathrm{f}-\frac{b\rho c_p V}{hA}[1-\exp(-hAt/(\rho c_p V))] \tag{23}$$

where b, ρ, c_p, V and A are all constant, and h is assumed to be immutability.

As stated in Section 4.1.3, the surface heat transfer coefficient is almost constant when the plate temperature is below 300 °C, and the plate temperature can be calculated directly in this condition. However, when the plate temperature is over 300 °C, the average surface heat transfer coefficient of different temperature ranges has to be used to give an approximate calculation. So, the equation is particularly suited to calculate the temperature of stepped heating.

5 Forecasting and validation

As shown in Fig. 1, if the gas temperature is heated directly to the treatment temperature, the plate temperature is far below the gas temperature, and hard to reach the target for a long time preservation. A feasible way is to heat the gas to a much higher temperature. In this method, high temperature difference between the gas and plate is preserved in the whole heating process, so the plate heating velocity is raised greatly.

To validate the method, a stepped solution treatment is designed, which is linearly heated-up step-by-step, as shown in Fig. 10. The heat treatment is divided into three steps: firstly, the plate is heated to 300 °C and preserved for 30 min; secondly, it is elevated to 400 °C and also preserved for 30 min; thirdly, the temperature is raised to 480 °C. To realize the treatment, the gas temperature is raised much higher than the heating temperature, and then cooled to the anticipate holding temperature rapidly. The key is the forecasting of the actual gas heating curve, and the difficulty is to find the peak value of every step shown in Fig. 10. Both the LPM and the finite element method (FEM) were carried out to forecast the gas heating curve. Then, according to the curve, the material and devices stated in Section 2 are used to measure the actual plate temperature.

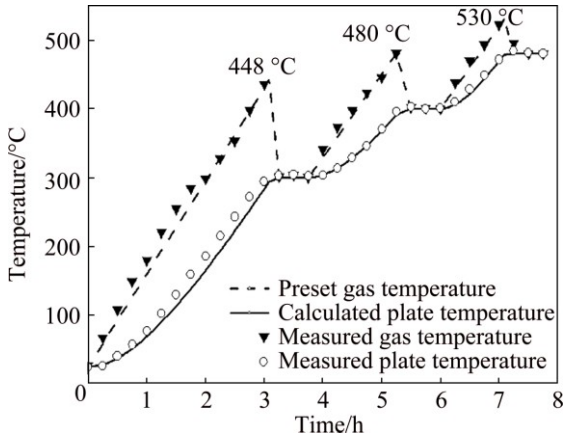

Fig. 10 Heating curves obtained by LPM and measurement

5.1 Lumped parameter method

The properties of 7050 thick plate shown in Fig. 2 are presented in Table 1. The gas heating velocities of the three steps are described in Table 2. The average surface heat transfer coefficients of the three steps are calculated by Eq. (18) and shown in Table 2. With these parameters, Eq. (23) was used directly for calculation. Then, the validation experiment is carried out with calculated gas temperature curve. The comparison is shown in Fig. 10.

Table 1 Properties of plate

Parameter	Value
Length/mm	1300
Width/mm	1100
Height/mm	180
Density/(kg·m^{-3})	2830
Specific heat capacity/(J·kg^{-1}·°C^{-1})	852
Thermal conductivity/(W·m^{-1}·°C^{-1})	157
Initial temperature/°C	25

Table 2 Gas heating velocity of three steps

Temperature range/°C	Heating velocity/ (°C·min^{-1})	Surface heat transfer coefficient/(W·m^{-2}·K^{-1})
25−300	2.25	37.5
300−400	2	47.5
400−480	2.375	67

A correlation coefficient (r) is used to evaluate the relationship between calculated result and the experimental data, which is calculated by

$$r=\frac{\sum(T_\mathrm{LPM}-\overline{T}_\mathrm{LPM})(T_\mathrm{M}-\overline{T}_\mathrm{M})}{\sqrt{\sum(T_\mathrm{LPM}-\overline{T}_\mathrm{LPM})^2\sum(T_\mathrm{M}-\overline{T}_\mathrm{M})^2}} \tag{24}$$

where T_LPM and $\overline{T}_\mathrm{LPM}$ are the temperature and the average temperature calculated by LPM, respectively; T_M and $\overline{T}_\mathrm{M}$ are the measured temperature and the average,

respectively. The calculated results fit with the experimental data better, when r approaches 1. And r is 0.998 calculated by Eq. (24), which indicates that the calculation result agrees well with the experimental data.

5.2 Finite element method

Using FEM to calculate the gas temperature curve is very complex. The plate temperature is easy to get by means of FEM from the gas temperature, but the inverse operation is very difficult. A common try-and-error method should be used to determine the gas temperature peak. After many trials, the gas temperature curve can be ascertained finally.

However, just for a comparison, the gas heating curve computed by the LPM in Section 5.1 is used directly for simulation. The simulation is carried out with the FEM software Abaqus 6.10™. The properties used are also shown in Table 1. The FEM domain is meshed with C3D8T elements. The surface heat transfer coefficient used is given by Eq. (18).

Then, the plate temperature is simulated, which also fits the expected temperature well. The temperature field contour at gas temperature of 448 °C shown in Fig. 11 is extracted. At this point, as the temperature difference between the gas and the plate is the largest, the maximum temperature difference will exist in the plate. As shown in Fig. 12, the simulated temperature is a little higher than the measured one. However, the temperature difference between the maximum and minimum is only 2.1 °C, especially when the thickness distribution is almost the same, which verifies the uniformity of the temperature again.

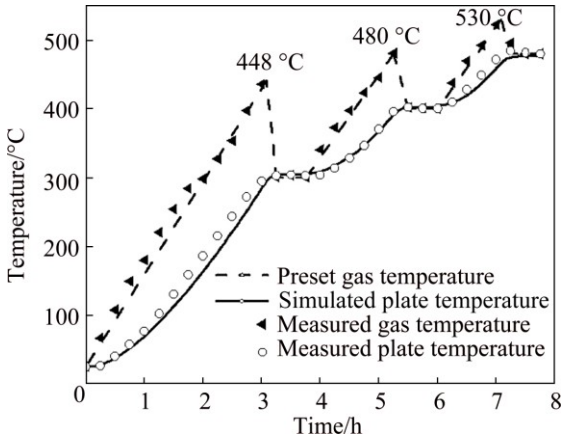

Fig. 11 Heating curves obtained by FEM and measurement

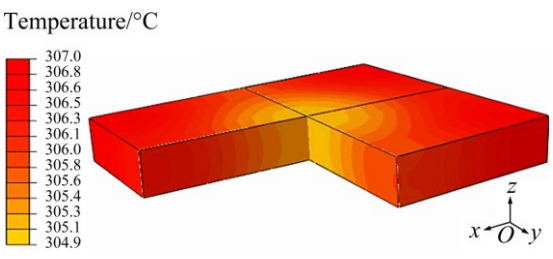

Fig. 12 Sectional contour of plate at the first temperature peak

In Fig. 13, heating curves of the FEM and LPM methods are in good agreement. At the temperature below 300 °C, the two methods give almost the same result, while there is a small difference when the temperature is above 300 °C, for the approximation of surface heat transfer coefficient in the LPM. However, the two methods are certified to be accurate by the results of experiment, and the LPM is quite simple and more effective than FEM.

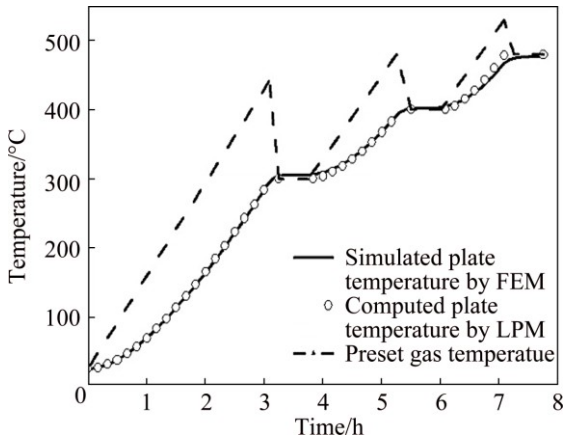

Fig. 13 Heating curves obtained by FEM and LPM

6 Conclusions

1) The temperature of aluminum thick plate (thickness below 180 mm) can be considered as uniform, which is validated by experimental and calculated results.

2) The relationship between the surface heat transfer coefficient and forced convection heat transfer and radiant heat transfer is discussed, and the calculated method of surface heat transfer coefficient using the transient plate temperature is given.

3) Based on the temperature uniformity of the plate, a convenient LPM is given to calculate the plate temperature, in which a stepped solution heat treatment is designed.

4) The validation of the design is carried out by FEM and experiment. Results show that the temperature results calculated by LPM and simulated by FEM agree well with the experimental data, and the LPM is apparently more convenient in engineering application.

References

[1] ROMETSCH P A, ZHANG Y, KNIGHT S. Heat treatment of 7xxx series aluminium alloys — Some recent developments [J]. Transactions of Nonferrous Metals Society of China, 2014, 24: 2003−2017.

[2] DANH N C, RAJAN K, WALLACE W. A TEM study of

microstructural changes during retrogression and reaging in 7075 aluminum [J]. Metallurgical Transactions A, 1983, 14: 1843−1850.
[3] MARLAUD T, DESCHAMPS A, BLEY F, LEFEBVRE W, BAROUX B. Evolution of precipitate microstructures during the retrogression and re-ageing heat treatment of an Al−Zn−Mg−Cu alloy [J]. Acta Materialia, 2010, 58: 4814−4826.
[4] URAL K. A study of optimization of heat-treatment conditions in retrogressions and re-ageing treatment of 7075-T6 aluminium alloy [J]. Journal of Materials Science Letters, 1994, 13: 383−385.
[5] OLIVEIRA A F, de BARROS M C, CARDOSO K R, TRAVESSA D N. The effect of RRA on the strength and SCC resistance on AA7050 and AA7150 aluminium alloys [J]. Materials Science and Engineering A, 2004, 379: 321−326.
[6] XIAO Yan-ping, PAN Qing-lin, LI Wen-bin, LIU Xiao-yan, HE Yun-bin. Influence of retrogression and re-aging treatment on corrosion behaviour of an Al−Zn−Mg−Cu alloy [J]. Materials & Design, 2011, 32: 2149−2156.
[7] LI Guo-feng, ZHANG Xin-ming, LI Peng-hui, YOU Jiang-hai. Effects of retrogression heating rate on microstructures and mechanical properties of aluminum alloy 7050 [J]. Transactions of Nonferrous Metals Society of China, 2010, 20: 935−941.
[8] RANGANATHA R, KUMAR V A, NANDI V S, BHAT R R, MURALIDHARA B K. Multi-stage heat treatment of aluminum alloy AA7049 [J]. Transactions of Nonferrous Metals Society of China, 2013, 23: 1570−1575.
[9] SONG Feng-xuan, ZHANG Xin-ming, LIU Sheng-dan, BAI Tan, HAN Nian-mei, TAN Ji-bo. Effects of solution heat treatment on microstructure and corrosion properties of 7050 Al alloy [J]. Journal of Aeronautical Materials, 2013, 4: 14−21. (in Chinese)
[10] LIU Sheng-dan, ZHANG Yong, LIU Wen-jun, DENG Yun-lai, ZHANG Xin-ming. Effect of step-quenching on microstructure of aluminum alloy 7055 [J]. Transactions of Nonferrous Metals Society of China, 2010, 20: 1−6.
[11] DENG Yun-lai, WAN Li, WU Li-hui, ZHANG Yun-ya, ZHANG Xin-ming. Microstructural evolution of Al−Zn−Mg−Cu alloy during homogenization [J]. Journal of Materials Science, 2011, 46: 875−881.
[12] CHEN Kang-hua, LIU Hong-wei, ZHANG Zhuo, LI Song, TODD R I. The improvement of constituent dissolution and mechanical properties of 7055 aluminum alloy by stepped heat treatments [J]. Journal of Materials Processing Technology, 2003, 142: 190−196.
[13] HAN Nian-mei, ZHANG Xin-ming, LIU Sheng-dan, HE Dao-guang, ZHANG Rong. Effect of solution treatment on the strength and fracture toughness of aluminum alloy 7050 [J]. Journal of Alloys and Compounds, 2011, 509: 4138−4145.
[14] XU D K, ROMETSCH P A, BIRBILIS N. Improved solution treatment for an as-rolled Al−Zn−Mg−Cu alloy. Part II: Microstructure and mechanical properties [J]. Materials Science and Engineering A, 2012, 534: 244−252.
[15] HOLMAN J P. Heat transfer [M]. New York: McGraw-hill, 1986.

超高强铝合金厚板升温温度场的计算与试验研究

范世通[1]，邓运来[1,2]，张 劲[3]，郭晓斌[1]

1. 中南大学 材料科学与工程学院，长沙 410083；
2. 中南大学 高性能与复杂制造国家重点实验室，长沙 410083；
3. 中南大学 轻合金研究院，长沙 410083

摘 要：采用多级热处理技术可以有效地提高铝合金厚板的力学性能和抗腐蚀性能，其工程应用的关键和难点是厚板温度的精确控制。基于工程尺寸厚板实测升温数据，研究厚板升温过程、表面换热系数计算方法和厚板温度预测方法。结果表明，升温过程中铝合金厚板表层和心部的温差很小。基于温度的均匀性，计算厚板的表面换热系数，表面换热系数在 300 °C 以下时为定值，但在 300 °C 以上升温时表面换热系数大幅上升。因此，开发了预测厚板温度的集总参数法，采用该方法设计多级固溶制度，并用有限元法和实测数据进行验证。采用集总参数法和有限元法计算的厚板升温曲线均与实测结果相符，且集总参数法在工程应用中更为便捷。

关键词：集总参数法；表面换热系数；温度场；铝合金；厚板

(Edited by Wei-ping CHEN)